Science of the Total Environment 633 (2018) 1360–1369

Contents lists available at ScienceDirect

Science of the Total Environment

journal homepage: www.elsevier.com/locate/scitotenv

Filter-based measurement of light absorption by brown carbon in $PM_{2.5}$ in a megacity in South China

Sheng Li [a,c], Ming Zhu [a,c], Weiqiang Yang [a,c], Mingjin Tang [a], Xueliang Huang [a], Yuegang Yu [a], Hua Fang [a,c], Xu Yu [a,c], Qingqing Yu [a,c], Xiaoxin Fu [d], Wei Song [a,b], Yanli Zhang [a,b], Xinhui Bi [a], Xinming Wang [a,b,c,*]

[a] State Key Laboratory of Organic Geochemistry, Guangdong Key Laboratory of Environmental Protection and Resources Utilization, Guangzhou Institute of Geochemistry, Chinese Academy of Sciences, Guangzhou 510640, China
[b] Center for Excellence in Regional Atmospheric Environment, Institute of Urban Environment, Chinese Academy of Sciences, Xiamen 361021, China
[c] University of Chinese Academy of Sciences, Beijing 100049, China
[d] School of Environment and Resource, Southwest University of Science and Technology, Mianyang 621010, China

HIGHLIGHTS

- Filter-based measurement of light absorption by BrC and BC.
- Larger seasonal variation of light absorption by BrC in rural sites.
- Biomass burning was a significant source of BrC in autumn.
- Secondary formation of BrC might be greater in summer than in autumn.
- Higher apparent MAE for EC at sites impacted by fossil fuel combustion.

GRAPHICAL ABSTRACT

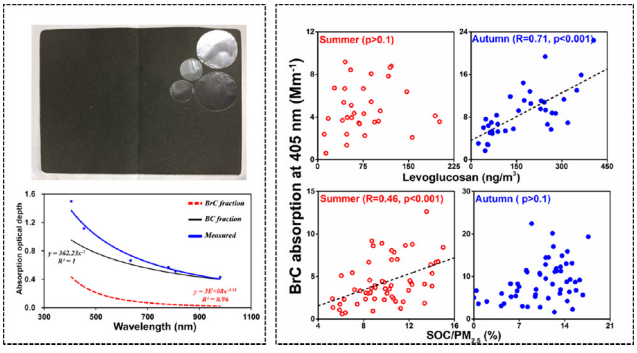

ARTICLE INFO

Article history:
Received 11 January 2018
Received in revised form 20 March 2018
Accepted 20 March 2018
Available online 3 April 2018

Editor: Jianmin Chen

Keywords:
Brown carbon
Black carbon
Elemental carbon
$PM_{2.5}$
Light absorption
Guangzhou

ABSTRACT

Carbonaceous aerosols represent an important nexus between air pollution and climate change. Here we collected filter-based $PM_{2.5}$ samples during summer and autumn in 2015 at one urban and two rural sites in Guangzhou, a megacity in southern China, and got the light absorption by black carbon (BC) and brown carbon (BrC) resolved with a DRI Model 2015 multi-wavelength thermal/optical carbon analyzer apart from determining the organic carbon (OC) and elemental carbon (EC) contents. On average BrC contributed 12–15% of the measured absorption at 405 nm (LA_{405}) during summer and 15–19% during autumn with significant increase in the LA_{405} by BrC at the rural sites. Carbonaceous aerosols, identified as total carbon (TC), yielded average mass absorption efficiency at 405 nm (MAE_{405}) that were approximately 45% higher in autumn than in summer, an 83% increase was noted in the average MAE_{405} for OC, compared with an increase of only 14% in the average MAE_{405} for EC. The LA_{405} by BrC showed a good correlation ($p < 0.001$) with the ratios of secondary OC to $PM_{2.5}$ in summer. However, this correlation was poor ($p > 0.1$) in autumn, implying greater secondary formation of BrC in summer. The correlations between levoglucosan (a marker of biomass burning) and the LA_{405} by BrC were significant during autumn but insignificant during summer, suggesting that the observed increase in the LA_{405} by BrC during autumn in rural areas was largely related to biomass burning. The measurements of light absorption at 550 nm presented in this study indicated that the use of the IMPROVE algorithm with an MAE value of

* Corresponding author.
E-mail address: wangxm@gig.ac.cn (X. Wang).

https://doi.org/10.1016/j.scitotenv.2018.03.235

10 m^2/g for EC to approximate light absorption may be appropriate in areas not strongly affected by fossil fuel combustion; however, this practice would underestimate the absorption of light by $PM_{2.5}$ in areas heavily affected by vehicle exhausts and coal burning.

1. Introduction

Atmospheric aerosols, which disperse globally but display significant regional variations, impact the radiative forcing received by the Earth both directly (by enhancing the scattering and absorption of solar radiation) and indirectly (through their important roles in cloud condensation and as ice nuclei) (Akimoto, 2003; Ramanathan et al., 2001). Carbonaceous aerosols, which represent an important part of atmospheric particulate matter, are very complex mixtures. They are typically divided into organic carbon (OC) and black carbon (BC) (Chung and Seinfeld, 2002). Many studies have demonstrated that carbonaceous aerosols are responsible for a large fraction of the light absorbed by airborne particles (Trijonis, 1982; Shah et al., 1984; Malm et al., 1994; Novakov et al., 1997). BC is considered to be the major carbonaceous aerosol component that efficiently absorbs visible (400–700 nm) light (Kirchstetter et al., 2004). Most OC absorbs light strongly in the infrared (IR) and ultraviolet (UV) ranges but is relatively transparent in the visible and near-IR ranges (Laskin et al., 2015). However, a number of recent studies have found that some types of OC can absorb light in UV–visible ranges (Andreae and Gelencser, 2006; Bond and Bergstrom, 2006; Ramanathan et al., 2007; Feng et al., 2013). These types of OC are termed brown carbon (BrC) (Pöschl, 2005; Andreae and Gelencser, 2006), which includes polycyclic aromatics, atmospheric humic-like substances (HULIS) and biopolymers. Field measurements suggest that BrC may contribute approximately 10–30% of the total absorption by carbonaceous aerosols at near-UV wavelength and approximately 10% at a wavelength of 550 nm (Bahadur et al., 2012; Lack et al., 2012; Washenfelder et al., 2015). BrC may even be responsible for >50% of the total light absorption at 370 nm and approximately 15% of the total light absorption at the middle wavelengths during biomass burning events (Favez et al., 2009). A global modeling study suggests that BrC could contribute up to $+0.25$ W m^{-2} or 19% of the absorption by anthropogenic aerosols (Feng et al., 2013). Consequently, the optical properties of BrC need to be explicitly included in models to accurately represent the radiative forcing produced by aerosols (Alexander et al., 2008).

BrC is relatively inefficient in absorbing light in the near-UV (300–400 nm) and visible ranges when compared to BC, and its efficiency decreases as the wavelength increases (Formenti et al., 2003; Kirchstetter et al., 2004; Andreae and Gelencser, 2006; Yang et al., 2009). BrC can originate from primary emissions, such as biomass and biofuel burning (Bond, 2001; Bergstrom et al., 2007; Laskin et al., 2015), and it can also be secondarily formed by multiphase reactions (Noziere et al., 2007; Noziere and Esteve, 2007; De Haan et al., 2009; De Haan et al., 2011; Nguyen et al., 2012; Lee et al., 2013; Drozd and McNeill, 2014; Powelson et al., 2014; Tang et al., 2016). Detailed characterization of BrC is difficult because of its inherent chemical complexity and the mixing state with other substances (Laskin et al., 2015).

Light absorption by BC and BrC can be differentiated by the absorption Angstörm exponent (AAE) values, assuming that the AAE values of BC (sometimes also termed elemental carbon or EC) are close to 1 (Bergstrom et al., 2002; Bond and Bergstrom, 2006; Drozd and McNeill, 2014). There are two ways to measure light absorption of BrC based on AAE values. One method involves direct measurements of the extinction and absorption coefficients of aerosol particles by instruments such as cavity ring-down spectroscopy (CRDS) (Scherer et al., 1997), cavity-enhanced absorption spectroscopy (CEAS) (Moosmuller et al., 2005; Washenfelder et al., 2013) and photoacoustic absorption spectrometer (PAAS) (Arnott et al., 1999; Flowers et al., 2010; Yuan et al., 2016). The second method involves measuring the transmission of light through particle-loaded filters to quantify aerosol optical properties using instruments including particle soot absorption photometer (PSAP) (Bond et al., 1999), multi-angle absorption photometer (MAAP) (Petzold and Schonlinner, 2004), multi-wavelength absorbance analyzer (MWAA) (Massabo et al., 2013), aethalometers (Hansen et al., 1984) and, most recently, multi-wavelength thermal/optical carbon analyzers (Chen et al., 2015).

The burning of biomass and biofuel contribute substantially to BrC (Gustafsson et al., 2009; Lack et al., 2012; Mohr et al., 2013; Liu et al., 2015; Mok et al., 2016), and nearly 3 billion people, mostly in developing countries, still burn various types of biomass to cook their food and heat their homes (Subramanian, 2014). Thus, the occurrence and effects of BrC from open and residential burning of biomass is also of increasing concern. However, data on airborne BrC in the densely populated developing countries, including China, are far from sufficient. It has been estimated that the annual mean atmospheric burden of BrC exceeds 4 mg m^{-2} in the eastern and southern regions of China (Feng et al., 2013). Field works also have shown that BrC contributed 10–30% to total aerosol light absorption in the Beijing-Tianjin-Hebei region in north China (Yang et al., 2009; Cheng et al., 2011; Du et al., 2014a, 2014b). In the Pearl River Delta (PRD) region, which is one of the world's largest megacities and lies in southern China, Yuan et al. (2016) recently measured the absorption of light by aerosol particles using a 3-wavelength photoacoustic soot spectrometer; the results suggest that BrC contributes >10% of the total aerosol light absorption at shorter wavelengths in this region. Considering the spatial and temporal imbalances in the sources and properties of BrC in the ambient air, field measurements intended to characterize BrC are urgently needed in China.

In this study, a DRI Model 2015 Multi-wavelength Carbon Analyzer was used to measure the light absorption by BrC in $PM_{2.5}$ collected on quartz filters at three sites (one urban site and two rural sites) in the PRD region. Although this off-line method does not evaluate the effects of particle size and morphology on the aerosol light absorption, it provides a simple and convenient means of measuring the light absorption of BrC based on the optical nature of the bulk particles on filters. The effects of the quartz filters on the measurements can be calculated and excluded using empirical formulas developed for thermal/optical analysis. This study focus on: 1) estimating the contributions by BrC to light absorption in a megacity in southern China using filter-based samples and 2) investigating the spatial and seasonal variations in the absorption of light by BrC as well as the factors that influence the amount of light it absorbs.

2. Sampling and analysis

2.1. Description of the sampling sites

The PRD region has become the largest urban area in the world in terms of both size and population (World Bank, 2015). The rapid growing industry and economy in the region has been accompanied by large emissions of primary pollutants (Chan and Yao, 2008), including light-absorbing BC and BrC, which have climatic effects. The region experiences a typical Asian monsoon climate; hot and humid conditions occur in the summer when the South China Sea monsoon is dominant, and relatively cool and dry conditions occur in the fall and winter, which feature prevailing northeasterly monsoon winds from northern China (Ding and Chan, 2005).

The three sampling sites in this work include one urban site in the city center (SZ; 23.13° N, 113.27° E) and two rural sites, one in the small town of Jiulong, which is located in the northeastern portion of Guangzhou (JL; 23.30° N, 113.57° E) and another in a small town of Wanqingsha in the central portion of the PRD (WQS; 22.71° N, 113.55° E). Their geographical locations are shown in Fig. 1. SZ and JL are two stations in the governmental ambient air quality monitoring network in Guangzhou, and the location of WQS enables the monitoring of the regional background air pollution in the PRD region. Detailed descriptions of the sampling sites can be found elsewhere (Zhang et al., 2012, 2013; Yu et al., 2016).

2.2. Sample collection

Field sampling was conducted from August 11 to August 31 (in the summer) and from November 1 to November 20 (in the autumn) in 2015. The 24-h $PM_{2.5}$ samples were collected simultaneously at the three sites using high-volume samplers (Tisch Environmental, Inc., OH, USA) with a constant flow rate of 1.1 m^3 min^{-1}. The $PM_{2.5}$ samples were collected on 20.3 × 25.4 cm quartz filters (Whatman, Mainstone, UK), which were pre-baked at 450 °C for 6 h before use.

2.3. Chemical analysis and light absorption measurement

Sulfate, nitrate and ammonium were analyzed with an ion chromatograph (883 Basic IC plus, Metrohm, Switzerland) (Fu et al., 2016). The detailed procedure for chemical analysis is given in Fu et al. (2015). Detailed procedures for the analysis of levoglucosan are described elsewhere (Yu et al., 2016). Briefly, filter samples were extracted by sonication with dichloride methane/methanol (1:1, v/v), and derivatized (silylation) with 100 μL of pyridine and 200 μL of *N,O*-bis-(trimethylsilyl)-trifluoroacetamide (BSTFA) plus 1% trimethylchlorosilane. The silylated extracts were analyzed by an Agilent 7890/5975C gas chromatography/mass spectrometer detector (GC/MSD) equipped with an HP-5 MS capillary column (30 m × 0.25 mm × 0.25 mm). For the measurements of OC and EC, a circular punch (0.8 cm in diameter) of each filter was taken and analyzed using a DRI Model 2015 multi-wavelength thermal/optical carbon analyzer (Desert Research Institute, Nevada, USA) with the IMPROVE_A protocol (Chow et al., 2007; Chow et al., 2011). Four OC fractions (OC1, OC2, OC3, and OC4 with cutting temperature of 140, 280, 480, and 580 °C, respectively, in a helium atmosphere) and three EC fractions (EC1, EC2, and EC3 with cutting temperature of 580, 740, and 840 °C, respectively, in a 2% oxygen/98% helium atmosphere). The detailed procedures for the OC/EC analysis are described in Chen et al. (2015).

Light absorption was also measured by the DRI Model 2015 multi-wavelength thermal/optical carbon analyzer. The analyzer equipped seven diode lasers with wavelengths of 405, 455, 532, 635, 780, 808 and 980 nm to monitor spectral reflectance and transmittance of filter samples. Since BrC is weak in absorbing infrared light, we chose the light absorption at 405, 455 and 635 nm for the discussion in this study (light absorption at 532 nm was not included due to in sufficient detector signal-to-noise ratio ratios) (Chen et al., 2015). Most previous studies have used transmittance attenuation (ATN) to estimate light absorption by particles on a filter:

$$ATN_\lambda = -\ln\left(\frac{FT_{\lambda,i}}{FT_{\lambda,f}}\right) \quad (1)$$

where $FT_{\lambda,i}$ and $FT_{\lambda,f}$ are the filter transmittance measured before and after thermal analysis, respectively; and $FT_{\lambda,f}$ approximates the transmittance of a blank filter. Due to filter effects, the absorption optical depth cannot be directly obtained from ATN at a given wavelength. Chen et al. (2015) argued that the relationship between the absorption optical depth τ_a and ATN is quadratic:

$$\tau_{a,\lambda} = A_\lambda \times ATN_\lambda^2 + B_\lambda \times ATN_\lambda \quad (2)$$

where $\tau_{a,\lambda}$ is the absorption optical depth at wavelength λ, and A_λ and B_λ are coefficients that include wavelength-specific multiple-scattering and loading effects. The values of A_λ and B_λ were reported in Chen et al. (2015). The relationship between $\tau_{a,\lambda}$ and ATN_λ could be applied to ambient samples to calculate $\tau_{a,\lambda}$ (Chen et al., 2015).

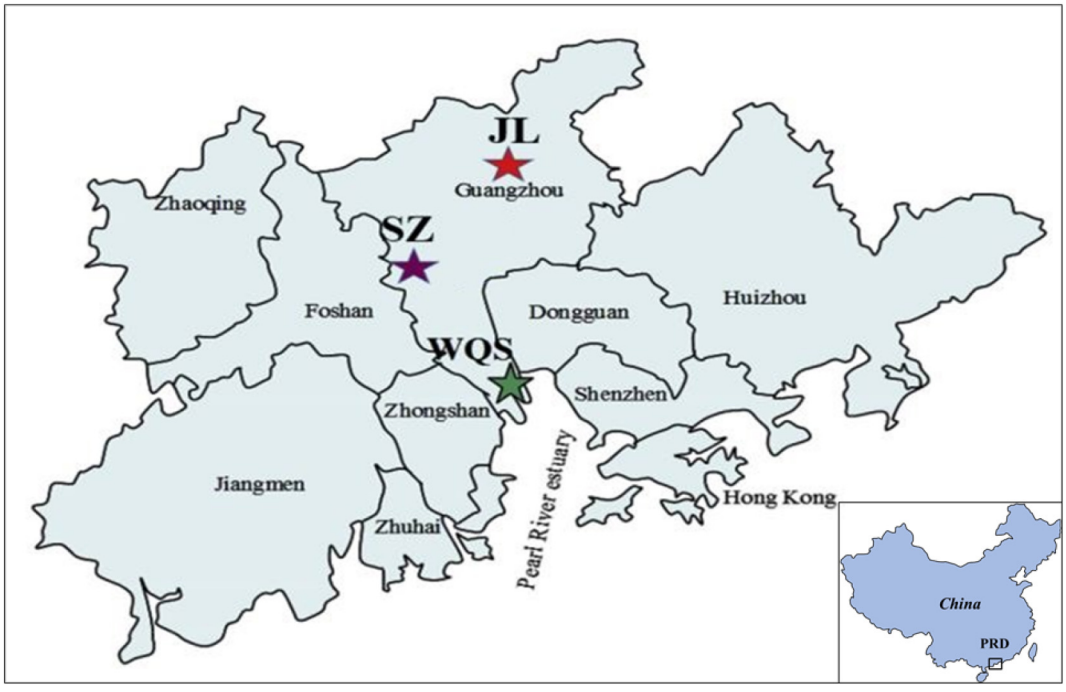

Fig. 1. Geographical locations of the three sampling sites (SZ, JL, and WQS) in the Pearl River Delta (PRD) region. The location of the PRD region in China is showed in the bottom right corner.

Since BC and BrC are the light-absorbing materials in aerosol samples, a simplified two-component model can be used to represent the optical absorption (Chen et al., 2015):

$$\tau_{a,\ \lambda} = K_{BC} \times \lambda^{-AAE_{BC}} + K_{BrC} \times \lambda^{-AAE_{BrC}} \quad (3)$$

where $\tau_{a,\lambda}$ is the absorption optical depth at wavelength λ; K_{BC} and K_{BrC} are the fitting coefficients for BC and BrC; and AAE_{BC} and AAE_{BrC} are the AAE values of BC and BrC, respectively. The absorption optical depths at a wavelength λ for BC and BrC ($\tau_{a,\lambda,BC}$ and $\tau_{a,\lambda,BrC}$, respectively) can be expressed as

$$\tau_{a,\ \lambda,BC} = K_{BC} \times \lambda^{-AAE_{BC}} \quad (4)$$

and

$$\tau_{a,\ \lambda,BrC} = K_{BrC} \times \lambda^{-AAE_{BrC}} \quad (5)$$

where $\tau_{a,\lambda,BC}$ and $\tau_{a,\lambda,BrC}$ are the absorption optical depths of BC and BrC, respectively, at a wavelength λ. In this study, we assume that AAE value of BC is equal to 1 (Bergstrom et al., 2002; Bond and Bergstrom, 2006; Drozd and McNeill, 2014). The fitting coefficients in Eq. (3) were obtained for AAE_{BrC} values between 2 and 8 by least-square linear regression, and the AAE_{BrC} that led to the best fit was selected as the valid AAE of BrC. As an example, the $\tau_{a,\lambda}$ decomposition as a function of wavelength from a sample collected at JL in summer was shown in Fig. 2. The ambient light absorption coefficient, b_{abs}, can be calculated using Eq. (6):

$$b_{abs} = \tau_{a,\lambda} \times \frac{A}{V} \quad (6)$$

where A is the filter area and V is the sampling volume. More detailed descriptions of the procedures and empirical formulas used are provided in Chen et al. (2015).

3. Results and discussion

3.1. Light absorption of $PM_{2.5}$

Time series of the total light absorption at three wavelengths (405, 455 and 635 nm) in different sites are shown in Fig. 3. During summer, the average total light absorption at 405, 455 and 635 nm were 44.0, 37.5 and 27.1 Mm^{-1} at SZ; 29.3, 25.4 and 17.9 Mm^{-1} at JL; and 20.9, 18.2 and 12.7 Mm^{-1} at WQS, respectively. During autumn, the average total light absorption at 405, 455 and 635 nm were 56.6, 47.8 and 32.8 Mm^{-1} at SZ, 56.3, 46.7 and 31.3 Mm^{-1} at JL and 44.9, 37.4 and 25.7 Mm^{-1} at WQS, respectively. These results are comparable to aerosol optical absorption values measured in the PRD region in 2014 by Yuan et al. (2016) using a 3-wavelength photoacoustic soot spectrometer. They observed that the average light absorption at 405 nm (LA_{405}) at Heshan (a rural site) was 32.5 Mm^{-1} from November 1 to November 22, whereas that at Shenzhen (an urban site) was 21.6 Mm^{-1} from September 12 to October 9 and 25.6 Mm^{-1} from January 15 to February 19 (Yuan et al., 2016).

Considering that BC plays a major role in the absorption of light by aerosols (Cappa et al., 2012; Chung et al., 2012; Bond et al., 2013), the total aerosol light absorption is expected to be largely controlled by the BC concentrations at the three sites. SZ is located in the city center, and anthropogenic emissions from vehicle exhaust and industrial activities there are the highest among the three sites examined in this study. More specifically, industrial activities and transportation have been estimated to account for 70% of the total BC emission in Guangzhou (Verma et al., 2010). Therefore, the average total light absorption at SZ was significantly higher than that at JL and WQS in summer. From summer to autumn, the aerosol LA_{405} by $PM_{2.5}$ increased by 38%, 92% and 115% at SZ, JL and WQS, respectively, which is partly attributed to the changes in atmospheric boundary layer height. However, the seasonal variations in the light absorption by $PM_{2.5}$ are more pronounced at the rural sites, suggesting that local emissions also contributed substantially in rural areas during the autumn. As pointed out by He et al. (2011), biomass burning emissions occur primarily in rural areas within the PRD regions and are greater in November than in August (Ding et al., 2012; Yu et al., 2016).

As shown in Fig. 3, higher $PM_{2.5}$ concentrations were not associated with higher total light absorption; for example, during period of August 20–28, when the $PM_{2.5}$ concentration reached its highest level, the absorption of light by $PM_{2.5}$ remained unchanged compared to that on normal days (Fig. 3a and b). This observation may be largely explained by increases in the proportion of scattering materials in the $PM_{2.5}$ during the period. Sulfate, nitrate and ammonium (SNA) are key components of PM that efficiently scatter visible radiation (Seinfeld and Pandis, 2006). As depicted in Fig. 3d and e, during this period, the mass ratios of SNA to $PM_{2.5}$ increased, whereas the mass ratios of secondary OC (SOC) to $PM_{2.5}$ decreased further. This result differs from the observations made by Yuan et al. (2016); in their results, the total absorption of light by $PM_{2.5}$ and the mass concentrations of organic aerosols display similar trends.

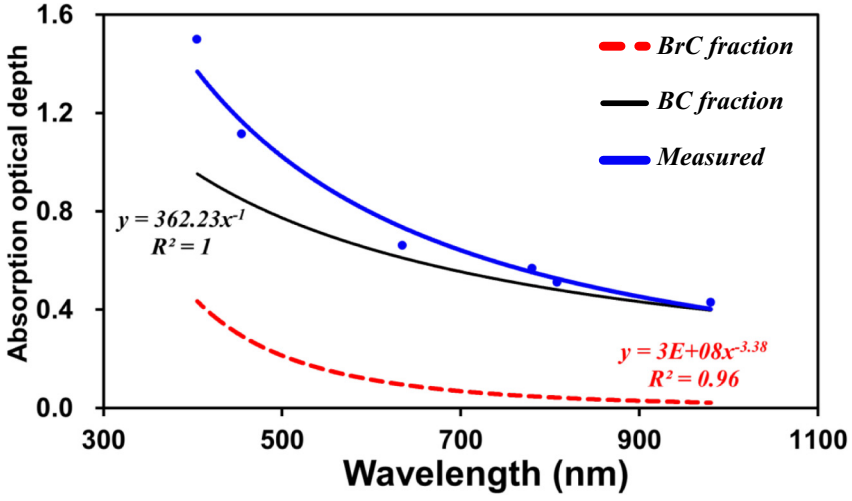

Fig. 2. An typical example showing the decomposition of measured absorption optical depth ($\tau_{a,\lambda}$) for a $PM_{2.5}$ filter sample from the JL site into the BC and BrC contributions based on their distinct spectral dependence of light absorption.

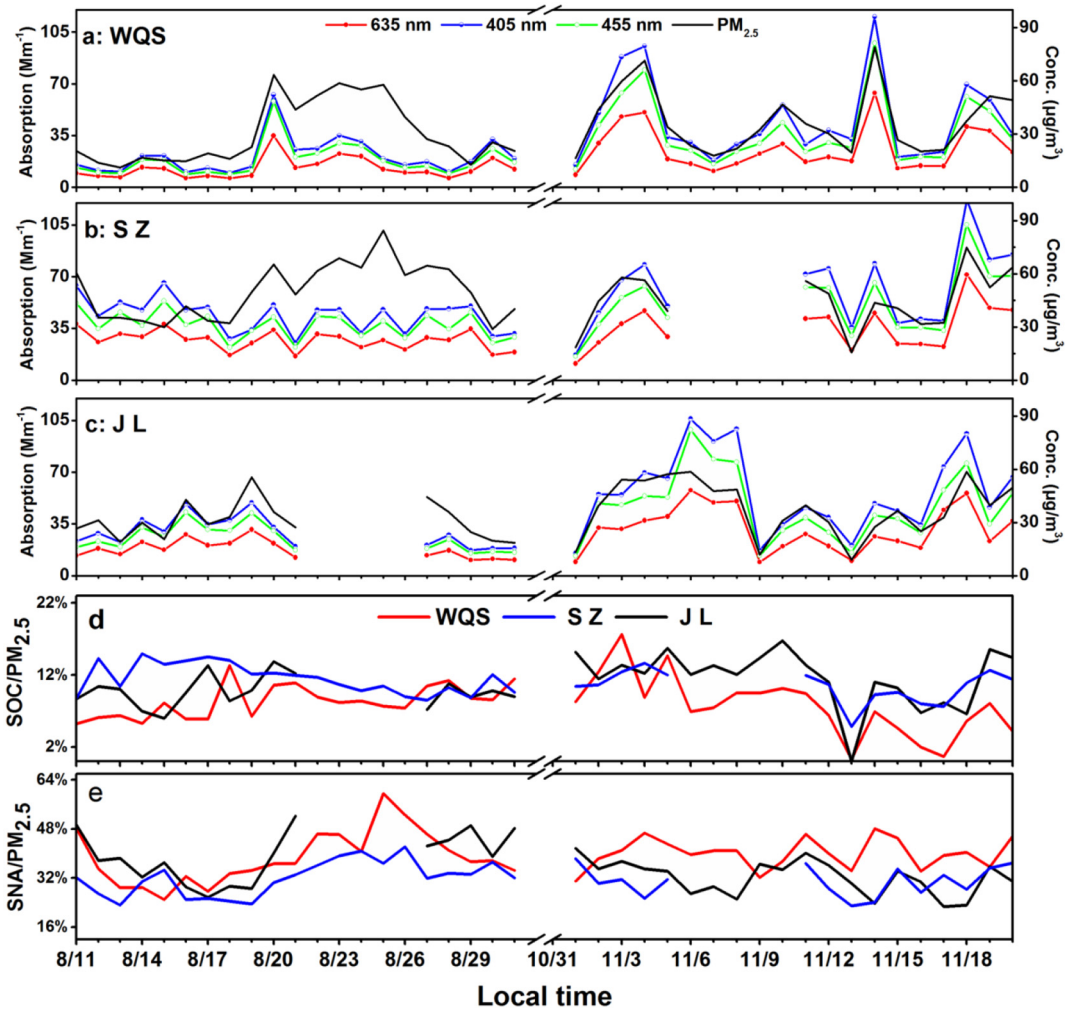

Fig. 3. The time series of $PM_{2.5}$ light absorption (a: WQS; b: SZ; c: JL) in comparison of that for mass ratios of SOC to $PM_{2.5}$ (d) and mass ratios of SNA (the sum of sulfate, nitrate and ammonium) to $PM_{2.5}$ (e).

3.2. Light absorption by BrC

Seasonal variations of the average LA_{405} by BrC at the three sites are shown in Fig. 4. During summer, the average LA_{405} by BrC was 6.4, 4.3 and 2.3 Mm^{-1} at SZ, JL and WQS, and BrC accounted for 14%, 15% and 12% of the total aerosol light absorption, respectively. During autumn, the average LA_{405} by BrC was 8.8, 9.9 and 8.8 Mm^{-1} at SZ, JL and WQS, and BrC accounted for 15%, 19% and 19% of the total aerosol light absorption, respectively. BC is the main light-absorbing material in both the rural and urban areas; however, the contribution of BrC to

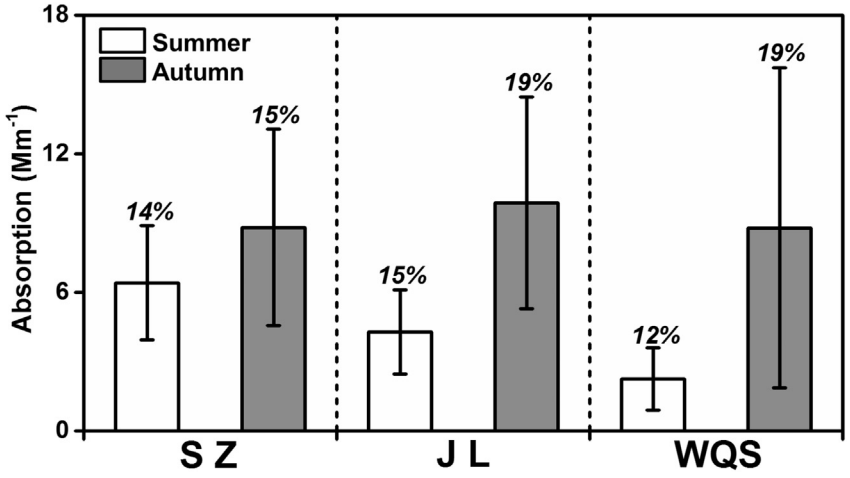

Fig. 4. Resolved average LA_{405} by BrC in the summer and autumn at the three sites. Error bar represent standard deviation (1σ). The percentages over the bars are contribution percentages of total absorption by BrC.

total aerosol light absorption was especially important at shorter wavelengths and during autumn. In autumn, BrC contributes nearly 20% of the total aerosol light absorption at the rural sites.

The absorption values of BrC were low and stable at site WQS in summer, likely because the air masses arriving at the site from the ocean driven by the summer monsoons were cleaner. At the urban site SZ, the average level of BrC was the highest of the three sites during the summer, which is attributable to the higher contribution of local emissions in this urban area. From summer to autumn, the average absorption values of BrC increased, which may be attributable to the lower boundary layer in autumn than in summer. However, as the increases at the rural sites were higher than that at the urban site, the emission sources at the rural sites are likely stronger, and biomass burning is a likely primary source (He et al., 2011). Previous studies have demonstrated that in rural areas of the PRD region, the concentrations of levoglucosan, a tracer of biomass burning, were significantly higher in autumn and winter when compared to those in the summer (Gao et al., 2011; Ding et al., 2012; Yu et al., 2016). Biomass burning is an important source of BrC (Gustafsson et al., 2009; Lack et al., 2012; Mohr et al., 2013; Liu et al., 2015; Mok et al., 2016), and it became the major source of polycyclic aromatic hydrocarbons, which are important components of BrC during the winter in Guangzhou (Yu et al., 2016). At site SZ, although the absorption by BrC increased from summer to autumn, its contributions to the total aerosol light absorption did not show a significant change. This site is mainly affected by local emissions in urban areas, and major sources for BC and BrC, including vehicle exhaust, industrial emissions and residential cooking, do not display significant seasonal variations.

A previous study conducted in the PRD region by Yuan et al. (2016) suggested that in autumn BrC contributed 6.3% of the LA_{405} at Shenzhen (an urban site) and 11.7% at Heshan (a rural site). The contributions by BrC to aerosol light absorption in other regions are similar to that in the PRD region. For example, BrC contributed ~30% of the total aerosol LA_{307} and ~10% of the total aerosol LA_{550} in Hebei, China (Yang et al., 2009), and BrC has been observed to account for ~10% of the LA_{405} in California, USA (Cappa et al., 2012). Generally, the contributions of BrC to light absorption are larger in background areas that are impacted to a greater degree by biomass burning. For example, the contributions of BrC to aerosol LA_{405} are as high as ~50% at Jeju, South Korea (Flowers et al., 2010) and 27 ± 15% (at 404 nm) in Boulder, Colorado, USA (Lack et al., 2012). Light absorption by dust was expected to be negligible and thus not considered in this study, because the contribution of carbonaceous materials to aerosol mass (>30%) is much larger than that of dust (<5%) (Huang et al., 2014).

3.3. Seasonal variation in the mass absorption efficiency of carbonaceous aerosols

As carbonaceous aerosols are the major light-absorbing component of $PM_{2.5}$ (Trijonis, 1982; Shah et al., 1984; Malm et al., 1994; Novakov et al., 1997), the total LA_{405} showed a highly significant ($p < 0.001$) correlation with total carbon (TC=OC + EC) in both summer and autumn (Fig. 5). However, the slope in summer (3.42 m^2/g) was lower than that in autumn (4.95 m^2/g), indicating that carbonaceous aerosols in autumn absorbed greater amounts of light and had higher mass absorption efficiency (MAE) value. The MAE of OC can be obtained by dividing the OC concentrations into the light absorption by BrC. The MAE of EC can be represented by the ratios of the light absorptions by BC to the EC concentrations.

The average MAE_{405} of EC was 11.8 m^2/g in summer, and this quantity increased by 13.6% to 13.4 m^2/g in autumn. However, the average MAE_{405} of OC increased by 83.1% from summer to autumn, when the MAE_{405} value were 0.7 m^2/g and 1.3 m^2/g, respectively. Therefore, the significant increase in the average MAE of OC was the major reason for the change in the average MAE of TC. The average $SOC/PM_{2.5}$ increased by only 0.03%, and the average $SNA/PM_{2.5}$ decreased by 1.8%. These results indicated that primary emissions, instead of secondary products, were probably the major contributors to the increase in the MAE of OC. The LA_{405} by BrC showed a fairly good correlation ($R = 0.71$, $p < 0.001$) with levoglucosan concentrations in autumn, but this correlation was insignificant in summer ($p > 0.1$) (Fig. 6), suggesting that biomass burning contributed more to BrC in autumn than in summer. A previous study has demonstrated that biomass burning-emitted BrC displays strong absorption at near-UV wavelengths (Lack et al., 2012); therefore, biomass burning may be a major source of BrC during the harvest seasons and has a significant effect on the enhancement of the light absorption by carbonaceous aerosols in the PRD region. As showed in Fig. 7, the correlation between the LA_{405} by BrC and the $SOC/PM_{2.5}$ ratios was significant in summer ($p < 0.001$) but insignificant in autumn ($p > 0.1$), indicating that secondary products had a greater effect on BrC in summer than in autumn although photobleaching effect would also be very strong in summer (Zhong and Jang, 2014).

3.4. Relationship between the light absorption by $PM_{2.5}$ and EC

The Interagency Monitoring of Protected Visual Environments (IMPROVE) project in the United States provides a simple method to estimate the light extinction coefficient of $PM_{2.5}$ (IMPROVE Report V,

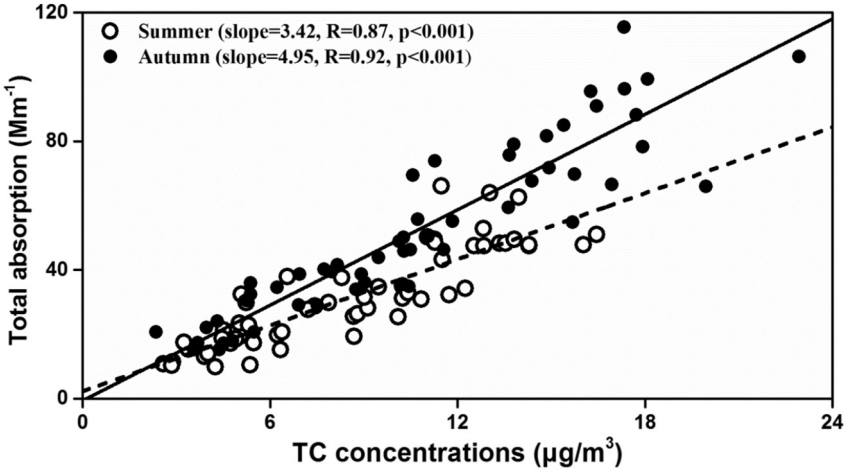

Fig. 5. Relationship between LA_{405} and TC concentrations measured with filter-based $PM_{2.5}$ samples during the summer and autumn in Guangzhou.

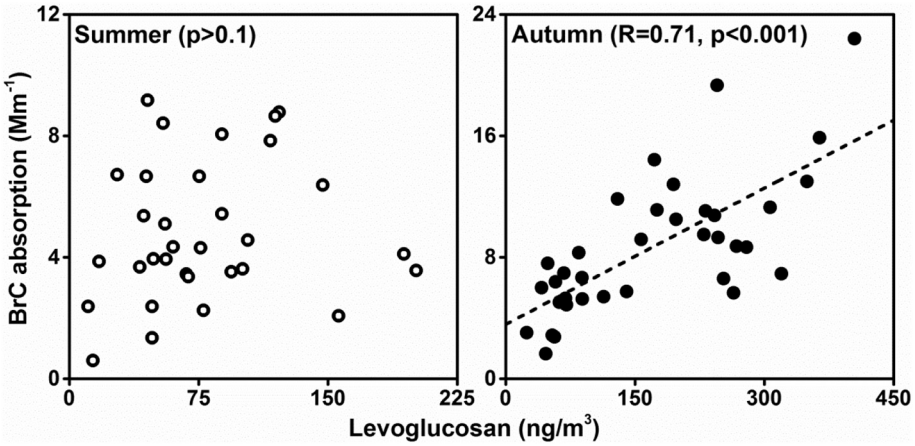

Fig. 6. Relationship between LA_{405} by BrC and levoglucosan concentrations during the summer and autumn in Guangzhou.

2011). The IMPROVE algorithm was used to calculate the light absorption by $PM_{2.5}$ with an MAE value of 10 m^2/g for EC (IMPROVE Report V, 2011). This MAE of EC corresponds to a wavelength of 550 nm (Hand and Malm, 2007). However, the MAE in the IMPROVE algorithm is only an approximation, and its application in some heavily polluted areas is under question (Fu et al., 2015).

The relationship between the LA_{550} by $PM_{2.5}$ and the EC concentrations at the three sites are shown in Fig. 8. The total absorption and EC concentrations are significantly correlated ($R = 0.94$, 0.91 and 0.98 at WQS, SZ and JL, respectively; $p < 0.001$) at all three sites (both of the rural sites and the urban site), suggesting that EC may, in fact, be a good indicator of the total light absorption by $PM_{2.5}$ in Guangzhou. However, the slopes at WQS, SZ and JL were 13.4, 12.8 and 10.1, respectively. As discussed in section 3.2, the average light absorption by BrC ranged from 12 to 19% of the total light absorption, and the contribution percentages were therefore quite similar at the three sites. Therefore, the different slopes may result largely from the different MAE values for EC at the three sites. According to previous studies, the MAE values of the EC from different sources vary and typically follow the order of wood burning < crop straw burning < vehicle emissions < coal briquette burning (Cheng et al., 2011; Shen et al., 2013; Xing et al., 2014). At site SZ in the city center, vehicle emissions may be the major source of EC. At site JL, which lies in a rural area surrounded by forests and farmlands, biomass burning there may make larger contributions to EC. Finally, site WQS is located in a small town in the central PRD region, and it is mainly affected by pollutants transported from surrounding industrial cities; the EC is derived largely from vehicle emissions and coal burning. These differences may explain why the slopes in Fig. 8 display in the order of WQS > SZ > JL. The slope at JL (10.1 m^2/g) was also the same as the 10 m^2/g for the MAE of EC used in the IMPROVE algorithm to estimate the light absorption by $PM_{2.5}$, and the slopes at WQS and SZ are approximately 30% higher. This result implies that, in areas less strongly affected by fossil fuel combustion, an MAE value of 10 m^2/g for EC can be used to estimate the light absorption by $PM_{2.5}$; however, the use of this value would underestimate the light absorption by $PM_{2.5}$ in urban and industrial areas.

4. Conclusion

A multi-wavelength thermal/optical carbon analyzer was used to determine OC/EC contents; further, the light absorption by the carbonaceous aerosols in filter-based $PM_{2.5}$ samples collected at one urban site and two rural sites in Guangzhou, a megacity in southern China, was characterized. The light absorptions by BC and BrC were differentiated. It is found that BrC could contribute 12–15% of the total aerosol light absorption at 405 nm during the summer, and 15–19% of that during the autumn. The average overall MAE at 405 nm for carbonaceous aerosols in terms of TC (OC + EC) increased by approximately 45% (from 3.42 m^2/g in summer to 4.95 m^2/g in autumn); the average MAE of EC at 405 nm increased by only approximately 14% (from 11.8 m^2/g in summer to 13.4 m^2/g in autumn) and the MAE_{405} of OC increased approximately 83% (from 0.7 m^2/g in summer to 1.3 m^2/g in autumn).

$SOC/PM_{2.5}$ ratios and the LA_{405} by BrC showed good correlations ($R = 0.46$, $p < 0.001$) in summer and poor correlations in autumn ($p > 0.1$), indicating that secondary products may have a greater impact on BrC in summer than in autumn. Instead, the LA_{405} by BrC showed a

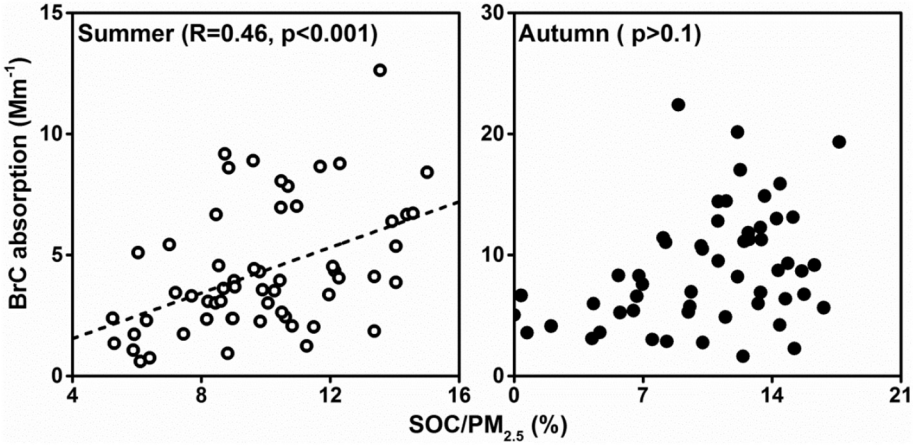

Fig. 7. Relationship between LA_{405} by BrC and $SOC/PM_{2.5}$ during the summer and autumn in Guangzhou.

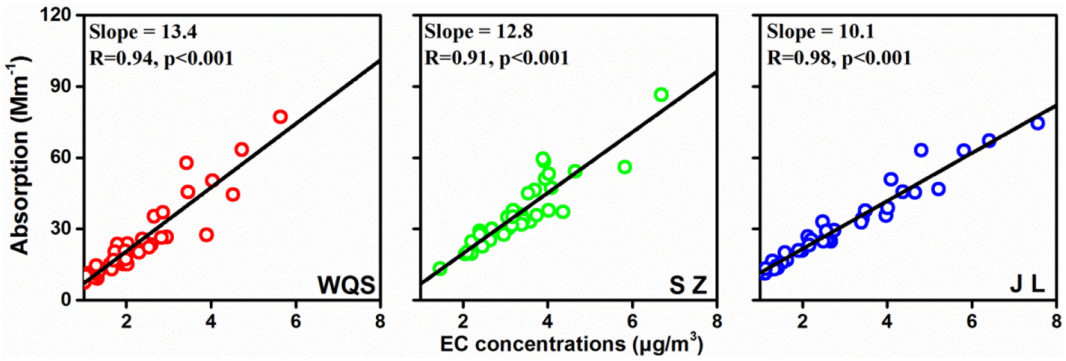

Fig. 8. Relationship between LA_{550} by $PM_{2.5}$ (calculated from the relationship between absorption and wavelength) and EC concentrations at the three sites in Guangzhou.

good correlation ($R = 0.71$, $p < 0.001$) with levoglucosan concentrations in autumn but a poor correlation ($p > 0.1$) in summer, suggesting that biomass burning contributes more to BrC in autumn.

The correlations between the total absorption at 550 nm and EC concentrations were highly significant at all of the studied sites, but the slopes of the total absorption at 550 nm to EC varied, due to the different sources of EC at the three sites. The MAE of 10 m^2/g used for EC in the IMPROVE algorithm is applicable in areas less affected by fossil fuel combustion, such as site JL; however, the use of this value and algorithm may result in underestimates of the light absorption by $PM_{2.5}$ in urban and industrial areas with greater contribution from fossil fuel (coal and oil) combustion, as is the case at sites WQS and SZ.

It should be noted that the filter-based method of estimating the light absorption by BrC in this study has limitations, as do alternative methods. Factors such as the size distribution of aerosol particles, their mixing state and particle morphology impact aerosol light absorption but are not taken into account in this filter-based method. Further field campaigns that include more comprehensive measurements of aerosol compositions, optical properties and other physicochemical properties are needed in order to better understand the effects of BrC in megacities.

Acknowledgements

This study was supported by the National Key Research and Development Program (2016YFC0202204), the Chinese Academy of Sciences (Grant No. QYZDJ-SSW-DQC032), the National Natural Science Foundation of China (Grant No. 41530641/41571130031/41673116/41603094), and the Guangzhou Science Technology and Innovation Commission (201607020002/201704020135).

References

Akimoto, H., 2003. Global air quality and pollution. Science 302:1716–1719. https://doi.org/10.1126/science.1092666.

Alexander, D.T.L., Crozier, P.A., Anderson, J.R., 2008. Brown carbon spheres in East Asian outflow and their optical properties. Science 321:833–836. https://doi.org/10.1126/science.1155296.

Andreae, M.O., Gelencser, A., 2006. Black carbon or brown carbon? The nature of light-absorbing carbonaceous aerosols. Atmos. Chem. Phys. 6:3131–3148. https://doi.org/10.5194/acp-6-3131-2006.

Arnott, W.P., Moosmuller, H., Rogers, C.F., Jin, T.F., Bruch, R., 1999. Photoacoustic spectrometer for measuring light absorption by aerosol: instrument description. Atmos. Environ. 33, 2845–2852.

Bahadur, R., Praveen, P.S., Xu, Y.Y., Ramanathan, V., 2012. Solar absorption by elemental and brown carbon determined from spectral observations. P. Natl. Acad. Sci. USA 109:17366–17371. https://doi.org/10.1073/pnas.1205910109.

Bergstrom, R.W., Russell, P.B., Hignett, P., 2002. Wavelength dependence of the absorption of black carbon particles: predictions and results from the TARFOX experiment and implications for the aerosol single scattering albedo. J. Atmos. Sci. 59, 567–577 http://dx.doi.org/10.1175/1520-0469(2002)059<0567:wdotao>2.0.co;2.

Bergstrom, R.W., Pilewskie, P., Russell, P.B., Redemann, J., Bond, T.C., Quinn, P.K., Sierau, B., 2007. Spectral absorption properties of atmospheric aerosols. Atmos. Chem. Phys. 7:5937–5943. https://doi.org/10.5194/acp-7-5937-2007.

Bond, T.C., 2001. Spectral dependence of visible light absorption by carbonaceous particles emitted from coal combustion. Geophys. Res. Lett. 28:4075–4078. https://doi.org/10.1029/2001GL013652.

Bond, T.C., Bergstrom, R.W., 2006. Light absorption by carbonaceous particles: an investigative review. Aerosol Sci. Technol. 40:27–67. https://doi.org/10.1080/02786820500421521.

Bond, T.C., Anderson, T.L., Campbell, D., 1999. Calibration and intercomparison of filter-based measurements of visible light absorption by aerosols. Aerosol Sci. Technol. 30:582–600. https://doi.org/10.1080/027868299304435.

Bond, T.C., Doherty, S.J., Fahey, D.W., Forster, P.M., Berntsen, T., DeAngelo, B.J., Flanner, M.G., Ghan, S., Karcher, B., Koch, D., Kinne, S., Kondo, Y., Quinn, P.K., Sarofim, M.C., Schultz, M.G., Schulz, M., Venkataraman, C., Zhang, H., Zhang, S., Bellouin, N., Guttikunda, S.K., Hopke, P.K., Jacobson, M.Z., Kaiser, J.W., Klimont, Z., Lohmann, U., Schwarz, J.P., Shindell, D., Storelvmo, T., Warren, S.G., Zender, C.S., 2013. Bounding the role of black carbon in the climate system: a scientific assessment. J. Geophys. Res. Atmos. 118:5380–5552. https://doi.org/10.1002/jgrd.50171.

Cappa, C.D., Onasch, T.B., Massoli, P., Worsnop, D.R., Bates, T.S., Cross, E.S., Davidovits, P., Hakala, J., Hayden, K.L., Jobson, B.T., Kolesar, K.R., Lack, D.A., Lerner, B.M., Li, S.M., Mellon, D., Nuaaman, I., Olfert, J.S., Petaja, T., Quinn, P.K., Song, C., Subramanian, R., Williams, E.J., Zaveri, R.A., 2012. Radiative absorption enhancements due to the mixing state of atmospheric black carbon. Science 337:1078–1081. https://doi.org/10.1126/science.1223447.

Chan, C.K., Yao, X., 2008. Air pollution in mega cities in China. Atmos. Environ. 42:1–42. https://doi.org/10.1016/j.atmosenv.2007.09.003.

Chen, L.W.A., Chow, J.C., Wang, X.L., Robles, J.A., Sumlin, B., Lowenthal, D.H., Zimmermann, R., Watson, J.G., 2015. Multi-wavelength optical measurement to enhance thermal/optical analysis for carbonaceous aerosol. Atmos. Meas. Tech. 8:451–461. https://doi.org/10.5194/amt-8-451-2015.

Cheng, Y., He, K.B., Zheng, M., Duan, F.K., Du, Z.Y., Ma, Y.L., Tan, J.H., Yang, F.M., Liu, J.M., Zhang, X.L., Weber, R.J., Bergin, M.H., Russell, A.G., 2011. Mass absorption efficiency of elemental carbon and water-soluble organic carbon in Beijing, China. Atmos. Chem. Phys. 11:11497–11510. https://doi.org/10.5194/acp-11-11497-2011.

Chow, J.C., Watson, J.G., Chen, L.W.A., Chang, M.C.O., Robinson, N.F., Trimble, D., Kohl, S., 2007. The IMPROVE-A temperature protocol for thermal/optical carbon analysis: maintaining consistency with a long-term database. J. Air Waste Manage. Assoc. 57:1014–1023. https://doi.org/10.3155/1047-3289.57.9.1014.

Chow, J.C., Watson, J.G., Robles, J., Wang, X., Chen, L.W.A., Trimble, D.L., Kohl, S.D., Tropp, R.J., Fung, K.K., 2011. Quality assurance and quality control for thermal/optical analysis of aerosol samples for organic and elemental carbon. Anal. Bioanal. Chem. 401:3141–3152. https://doi.org/10.1007/s00216-011-5103-3.

Chung, S.H., Seinfeld, J.H., 2002. Global distribution and climate forcing of carbonaceous aerosols. J. Geophys. Res. Atmos. 107:33. https://doi.org/10.1029/2001jd001397.

Chung, C.E., Ramanathan, V., Decremer, D., 2012. Observationally constrained estimates of carbonaceous aerosol radiative forcing. P. Natl. Acad. Sci. USA 109:11624–11629. https://doi.org/10.1073/pnas.1203707109.

De Haan, D.O., Corrigan, A.L., Tolbert, M.A., Jimenez, J.L., Wood, S.E., Turley, J.J., 2009. Secondary organic aerosol formation by self-reactions of methylglyoxal and glyoxal in evaporating droplets. Environ. Sci. Technol. 43:8184–8190. https://doi.org/10.1021/es902152t.

De Haan, D.O., Hawkins, L.N., Kononenko, J.A., Turley, J.J., Corrigan, A.L., Tolbert, M.A., Jimenez, J.L., 2011. Formation of nitrogen-containing oligomers by methylglyoxal and amines in simulated evaporating cloud droplets. Environ. Sci. Technol. 45:984–991. https://doi.org/10.1021/es102933x.

Ding, Y.H., Chan, J.C.L., 2005. The East Asian summer monsoon: an overview. Meteorog. Atmos. Phys. 89:117–142. https://doi.org/10.1007/s00703-005-0125-z.

Ding, X., Wang, X.M., Gao, B., Fu, X.X., He, Q.F., Zhao, X.Y., Yu, J.Z., Zheng, M., 2012. Tracer-based estimation of secondary organic carbon in the Pearl River Delta, south China. J. Geophys. Res. Atmos. 117. https://doi.org/10.1029/2011jd016596.

Drozd, G.T., McNeill, V.F., 2014. Organic matrix effects on the formation of light-absorbing compounds from alpha-dicarbonyls in aqueous salt solution. Environ. Sci.: Processes Impacts 16:741–747. https://doi.org/10.1039/c3em00579h.

Du, Z., He, K., Cheng, Y., Duan, F., Ma, Y., Liu, J., Zhang, X., Zheng, M., Weber, R., 2014a. A yearlong study of water-soluble organic carbon in Beijing I: sources and its primary vs. secondary nature. Atmos. Environ. 92:514–521. https://doi.org/10.1016/j.atmosenv.2014.04.060.

Du, Z., He, K., Cheng, Y., Duan, F., Ma, Y., Liu, J., Zhang, X., Zheng, M., Weber, R., 2014b. A yearlong study of water-soluble organic carbon in Beijing II: light absorption properties. Atmos. Environ. 89:235–241. https://doi.org/10.1016/j.atmosenv.2014.02.022.

Favez, O., Alfaro, S.C., Sciare, J., Cachier, H., Abdelwahab, M.M., 2009. Ambient measurements of light-absorption by agricultural waste burning organic aerosols. J. Aerosol Sci. 40:613–620. https://doi.org/10.1016/j.jaerosci.2009.04.002.

Feng, Y., Ramanathan, V., Kotamarthi, V.R., 2013. Brown carbon: a significant atmospheric absorber of solar radiation? Atmos. Chem. Phys. 13:8607–8621. https://doi.org/10.5194/acp-13-8607-2013.

Flowers, B.A., Dubey, M.K., Mazzoleni, C., Stone, E.A., Schauer, J.J., Kim, S.W., Yoon, S.C., 2010. Optical-chemical-microphysical relationships and closure studies for mixed carbonaceous aerosols observed at Jeju Island; 3-laser photoacoustic spectrometer, particle sizing, and filter analysis. Atmos. Chem. Phys. 10:10387–10398. https://doi.org/10.5194/acp-10-10387-2010.

Formenti, P., Elbert, W., Maenhaut, W., Haywood, J., Osborne, S., Andreae, M.O., 2003. Inorganic and carbonaceous aerosols during the southern African regional science initiative (SAFARI 2000) experiment: chemical characteristics, physical properties, and emission data for smoke from African biomass burning. J. Geophys. Res. Atmos. 108. https://doi.org/10.1029/2002JD002408.

Fu, X., Guo, H., Wang, X., Ding, X., He, Q., Liu, T., Zhang, Z., 2015. $PM_{2.5}$ acidity at a background site in the Pearl River Delta region in fall-winter of 2007-2012. J. Hazard. Mater. 286:484–492. https://doi.org/10.1016/j.jhazmat.2015.01.022.

Fu, X.X., Wang, X.M., Hu, Q.H., Li, G.H., Ding, X., Zhang, Y.L., He, Q.F., Liu, T.Y., Zhang, Z., Yu, Q.Q., Shen, R.Q., Bi, X.H., 2016. Changes in visibility with $PM_{2.5}$ composition and relative humidity at a background site in the Pearl River Delta region. J. Environ. Sci. 40:10–19. https://doi.org/10.1016/j.jes.2015.12.001.

Gao, B., Yu, J.Z., Li, S.X., Ding, X., He, Q.F., Wang, X.M., 2011. Roadside and rooftop measurements of polycyclic aromatic hydrocarbons in $PM_{2.5}$ in urban Guangzhou: evaluation of vehicular and regional combustion source contributions. Atmos. Environ. 45:7184–7191. https://doi.org/10.1016/j.atmosenv.2011.09.005.

Gustafsson, O., Kruså, M., Zencak, Z., Sheesley, R.J., Granat, L., Engström, E., Praveen, P.S., Rao, P.S., Leck, C., Rodhe, H., 2009. Brown clouds over South Asia: biomass or fossil fuel combustion? Science 323:495–498. https://doi.org/10.1126/science.1164857.

Hand, J.L., Malm, W.C., 2007. Review of aerosol mass scattering efficiencies from ground-based measurements since 1990. J. Geophys. Res.-Atmos. 112 (D18). https://doi.org/10.1029/2007JD008484.

Hansen, A.D.A., Rosen, H., Novakov, T., 1984. The aethalometer – an instrument for the real-time measurement of optical-absorption by aerosol-particals. Sci. Total Environ. 36:191–196. https://doi.org/10.1016/0048-9697(84)90265-1.

He, M., Zheng, J.Y., Yin, S.S., Zhang, Y.Y., 2011. Trends, temporal and spatial characteristics, and uncertainties in biomass burning emissions in the Pearl River Delta, China. Atmos. Environ. 45:4051–4059. https://doi.org/10.1016/j.atmosenv.2011.04.016.

Huang, X., Yun, H., Gong, Z., Li, X., He, L., Zhang, Y., Hu, M., 2014. Source apportionment and secondary organic aerosol estimation of $PM_{2.5}$ in an urban atmosphere in China. Sci. China Earth Sci. 57:1352–1362. https://doi.org/10.1007/s11430-013-4686-2.

IMPROVE (Interagency Monitoring of Protected Visual Environments) Report V, 2011. Spatial and seasonal patterns and temporal variability of haze and its constituents in the United States. Cooperative Institute for Research in the Atmosphere. Colorado State University, Colorado, USA.

Kirchstetter, T.W., Novakov, T., Hobbs, P.V., 2004. Evidence that the spectral dependence of light absorption by aerosols is affected by organic carbon. J. Geophys. Res. Atmos. 109:12. https://doi.org/10.1029/2004JD004999.

Lack, D.A., Langridge, J.M., Bahreini, R., Cappa, C.D., Middlebrook, A.M., Schwarz, J.P., 2012. Brown carbon and internal mixing in biomass burning particles. P. Natl. Acad. Sci. USA 109:14802–14807. https://doi.org/10.1073/pnas.1206575109.

Laskin, A., Laskin, J., Nizkorodov, S.A., 2015. Chemistry of atmospheric brown carbon. Chem. Rev. 115:4335–4382. https://doi.org/10.1021/cr5006167.

Lee, A.K.Y., Zhao, R., Li, R., Liggio, J., Li, S.M., Abbatt, J.P.D., 2013. Formation of light absorbing organo-nitrogen species from evaporation of droplets containing glyoxal and ammonium sulfate. Environ. Sci. Technol. 47:12819–12826. https://doi.org/10.1021/es402687w.

Liu, S., Aiken, A.C., Gorkowski, K., Dubey, M.K., Cappa, C.D., Williams, L.R., Herndon, S.C., Massoli, P., Fortner, E.C., Chhabra, P.S., Brooks, W.A., Onasch, T.B., Jayne, J.T., Worsnop, D.R., China, S., Sharma, N., Mazzoleni, C., Xu, L., Ng, N.L., Liu, D., Allan, J.D., Lee, J.D., Fleming, Z.L., Mohr, C., Zotter, P., Szidat, S., Prevot, A.S.H., 2015. Enhanced light absorption by mixed source black and brown carbon particles in UK winter. Nat. Commun. 6 (10). https://doi.org/10.1038/ncomms9435.

Malm, W.C., Sisler, J.F., Huffman, D., Eldred, R.A., Cahill, T.A., 1994. Spatial and seasonal trends in particle concentration and optical extinction in the United States. J. Geophys. Res. Atmos. 99:1347–1370. https://doi.org/10.1029/93jd02916.

Massabo, D., Bernardoni, V., Bove, M.C., Brunengo, A., Cuccia, E., Piazzalunga, A., Prati, P., Valli, G., Vecchi, R., 2013. A multi-wavelength optical set-up for the characterization of carbonaceous particulate matter. J. Aerosol Sci. 60:34–46. https://doi.org/10.1016/j.jaerosci.2013.02.006.

Mohr, C., Lopez-Hilfiker, F.D., Zotter, P., Prevot, A.S.H., Xu, L., Ng, N.L., Herndon, S.C., Williams, L.R., Franklin, J.P., Zahniser, M.S., Worsnop, D.R., Knighton, W.B., Aiken, A.C., Gorkowski, K.J., Dubey, M.K., Allan, J.D., Thornton, J.A., 2013. Contribution of nitrated phenols to wood burning brown carbon light absorption in Detling, United Kingdom during winter time. Environ. Sci. Technol. 47:6316–6324. https://doi.org/10.1021/es400683v.

Mok, J., Krotkov, N.A., Arola, A., Torres, O., Jethva, H., Andrade, M., Labow, G., Eck, T.F., Li, Z., Dickerson, R.R., Stenchikov, G.L., Osipov, S., Ren, X., 2016. Impacts of brown carbon from biomass burning on surface UV and ozone photochemistry in the Amazon Basin. Sci. Rep. 6. https://doi.org/10.1038/srep36940.

Moosmuller, H., Varma, R., Arnott, W.P., 2005. Cavity ring-down and cavity-enhanced detection techniques for the measurement of aerosol extinction. Aerosol Sci. Technol. 39:30–39. https://doi.org/10.1080/027868290903880.

Nguyen, T.B., Lee, P.B., Updyke, K.M., Bones, D.L., Laskin, J., Laskin, A., Nizkorodov, S.A., 2012. Formation of nitrogen- and sulfur-containing light-absorbing compounds accelerated by evaporation of water from secondary organic aerosols. J. Geophys. Res. Atmos. 117. https://doi.org/10.1029/2011jd016944.

Novakov, T., Hegg, D.A., Hobbs, P.V., 1997. Airborne measurements of carbonaceous aerosols on the East Coast of the United States. J. Geophys. Res. Atmos. 102:30023–30030. https://doi.org/10.1029/97jd02793.

Noziere, B., Esteve, W., 2007. Light-absorbing aldol condensation products in acidic aerosols: spectra, kinetics, and contribution to the absorption index. Atmos. Environ. 41:1150–1163. https://doi.org/10.1016/j.atmosenv.2006.10.001.

Noziere, B., Dziedzic, P., Cordova, A., 2007. Formation of secondary light-absorbing "fulvic-like" oligomers: a common process in aqueous and ionic atmospheric particles? Geophys. Res. Lett. 34. https://doi.org/10.1029/2007gl031300.

Petzold, A., Schonlinner, M., 2004. Multi-angle absorption photometry - a new method for the measurement of aerosol light absorption and atmospheric black carbon. J. Aerosol Sci. 35:421–441. https://doi.org/10.1016/j.jaerosci.2003.09.005.

Pöschl, U., 2005. Atmospheric aerosols: composition, transformation, climate and health effects. Angew. Chem. Int. Ed. 44:7520–7540. https://doi.org/10.1002/anie.200501122.

Powelson, M.H., Espelien, B.M., Hawkins, L.N., Galloway, M.M., De Haan, D.O., 2014. Brown carbon formation by aqueous-phase carbonyl compound reactions with amines and ammonium sulfate. Environ. Sci. Technol. 48:985–993. https://doi.org/10.1021/es4038325.

Ramanathan, V., Crutzen, P.J., Kiehl, J.T., Rosenfeld, D., 2001. Aerosols, climate, and the hydrological cycle. Science 294:2119–2124. https://doi.org/10.1126/science.1064034.

Ramanathan, V., Li, F., Ramana, M.V., Praveen, P.S., Kim, D., Corrigan, C.E., Nguyen, H., Stone, E.A., Schauer, J.J., Carmichael, G.R., 2007. Atmospheric brown clouds: hemispherical and regional variations in long-range transport, absorption, and radiative forcing. J. Geophys. Res. Atmos. 112:365–371 D22S21. https://doi.org/10.1029/2006JD008124.

Scherer, J.J., Paul, J.B., Okeefe, A., Saykally, R.J., 1997. Cavity ringdown laser absorption spectroscopy: history, development, and application to pulsed molecular beams. Chem. Rev. 97:25–51. https://doi.org/10.1021/cr930048d.

Seinfeld, J.H., Pandis, S.N., 2006. Atmospheric Chemistry and Physical: From Air Pollution to Climate Change. John Wiley & Sons, New York, pp. 691–719.

Shah, J.J., Watson, J.G., Cooper, J.A., Huntzicker, J.J., 1984. Aerosol chemical-composition and light-scattering in Portland, Oregon – the role of carbon. Atmos. Environ. 18:235–240. https://doi.org/10.1016/0004-6981 (84)90249-X.

Shen, G., Chen, Y., Wei, S., Fu, X., Zhu, Y., Tao, S., 2013. Mass absorption efficiency of elemental carbon for source samples from residential biomass and coal combustions. Atmos. Environ. 79:79–84. https://doi.org/10.1016/j.atmosenv.2013.05.082.

Subramanian, M., 2014. Deadly dinners. Nature 509:548–551. https://doi.org/10.1038/509548a.

Tang, M.J., Alexander, J.M., Kwon, D., Estillore, A.D., Laskina, O., Young, M.A., Kleiber, P.D., Grassian, V.H., 2016. Optical and physicochemical properties of brown carbon aerosol: light scattering, FTIR extinction spectroscopy, and hygroscopic growth. J. Phys. Chem. A 120:4155–4166. https://doi.org/10.1021/acs.jpca.6b03425.

Trijonis, J., 1982. Existing and natural background levels of visibility and fine particles in the rural East. Atmos. Environ. 16:2431–2445. https://doi.org/10.1016/0004-6981(82)90133-0.

Verma, R.L., Sahu, L.K., Kondo, Y., Takegawa, N., Han, S., Jung, J.S., Kim, Y.J., Fan, S., Sugimoto, N., Shammaa, M.H., Zhang, Y.H., Zhao, Y., 2010. Temporal variations of black carbon in Guangzhou, China, in summer 2006. Atmos. Chem. Phys. 10:6471–6485. https://doi.org/10.5194/acp-10-6471-2010.

Washenfelder, R.A., Flores, J.M., Brock, C.A., Brown, S.S., Rudich, Y., 2013. Broadband measurements of aerosol extinction in the ultraviolet spectral region. Atmos. Meas. Tech. 6:861–877. https://doi.org/10.5194/amt-6-861-2013.

Washenfelder, R.A., Attwood, A.R., Brock, C.A., Guo, H., Xu, L., Weber, R.J., Ng, N.L., Allen, H.M., Ayres, B.R., Baumann, K., Cohen, R.C., Draper, D.C., Duffey, K.C., Edgerton, E., Fry, J.L., Hu, W.W., Jimenez, J.L., Palm, B.B., Romer, P., Stone, E.A., Wooldridge, P.J., Brown, S.S., 2015. Biomass burning dominates brown carbon absorption in the rural southeastern United States. Geophys. Res. Lett. 42:653–664. https://doi.org/10.1002/2014gl062444.

World Bank, 2015. East Asia's changing urban landscape: measuring a decade of spatial growth. Urban Development Series. World Bank Group, Washington, DC.

Xing, Z.Y., Deng, J.J., Mu, C., Wang, Y., Du, K., 2014. Seasonal variation of mass absorption efficiency of elemental carbon in the four major emission areas in China. Aerosol Air Qual. Res. 14 1897-U1135. https://doi.org/10.4209/aaqr.2014.06.0121.

Yang, M., Howell, S.G., Zhuang, J., Huebert, B.J., 2009. Attribution of aerosol light absorption to black carbon, brown carbon, and dust in China - interpretations of atmospheric measurements during EAST-AIRE. Atmos. Chem. Phys. 9:2035–2050. https://doi.org/10.5194/acp-9-2035-2009.

Yu, Q.Q., Gao, B., Li, G.H., Zhang, Y.L., He, Q.F., Deng, W., Huang, Z.H., Ding, X., Hu, Q.H., Huang, Z.Z., Wang, Y.J., Bi, X.H., Wang, X.M., 2016. Attributing risk burden of $PM_{2.5}$-bound polycyclic aromatic hydrocarbons to major emission sources: case study in Guangzhou, South China. Atmos. Environ. 142:313–323. https://doi.org/10.1016/j.atmosenv.2016.08.009.

Yuan, J.F., Huang, X.F., Cao, L.M., Cui, J., Zhu, Q., Huang, C.N., Lan, Z.J., He, L.Y., 2016. Light absorption of brown carbon aerosol in the PRD region of China. Atmos. Chem. Phys. 16:1433–1443. https://doi.org/10.5194/acp-16-1433-2016.

Zhang, Y.L., Wang, X.M., Blake, D.R., Li, L.F., Zhang, Z., Wang, S.Y., Guo, H., Lee, F.S.C., Gao, B., Chan, L.Y., Wu, D., Rowland, F.S., 2012. Aromatic hydrocarbons as ozone precursors

before and after outbreak of the 2008 financial crisis in the Pearl River Delta region, south China. J. Geophys. Res. Atmos. 117:16. https://doi.org/10.1029/2011jd017356.
Zhang, Y., Wang, X., Barletta, B., Simpson, I.J., Blake, D.R., Fu, X., Zhang, Z., He, Q., Liu, T., Zhao, X., Ding, X., 2013. Source attributions of hazardous aromatic hydrocarbons in urban, suburban and rural areas in the Pearl River Delta (PRD) region. J. Hazard. Mater. 250:403–411. https://doi.org/10.1016/j.jhazmat 2013.02.023.
Zhong, M., Jang, M., 2014. Dynamic light absorption of biomass-burning organic carbon photochemically aged under natural sunlight. Atmos. Chem. Phys. 14:1517–1525. https://doi.org/10.5194/acp-14-1517-2014.